TOURO COLLEGE & UNIVERSITY SYSTEM

Touro Scholar

College of Pharmacy (TUC) Publications and Research

College of Pharmacy

2015

In Planta Production of Flock House Virus Transencapsidated RNA and Its Potential Use as a Vaccine

Yiyang Zhou

Payal D. Maharaj
Touro University California, payal.maharaj@tu.edu

Jyothi K. Mallajosyula
Touro University California, jyothi.mallajosyula@tu.edu

Alison A. McCormick
Touro University California, alison.mccormick@tu.edu

Christopher M. Kearney

Follow this and additional works at: https://touroscholar.touro.edu/tuccop_pubs

Part of the Pharmaceutics and Drug Design Commons

Recommended Citation

1   *In planta* production of *Flock House virus* trans-encapsidated RNA and its

2   potential use as a vaccine

3

4

5   Yiyang Zhou[a], Payal D. Maharaj, Jyothi K. Mallajosyula, Alison A.

6   McCormick[b], Christopher M. Kearney[a,c]#

7

8   Biomedical Studies Program[a] and Department of Biology[c], Baylor University, Waco,

9   Texas, USA;

10   Touro University California, College of Pharmacy, Vallejo CA, USA[b]

11

12

13   Running Head: *In planta* transencapsidated Flock House virus nanoparticle

14

15   #Address correspondence to Christopher Kearney, chris_kearney@baylor.edu

16

18

19

20

21   Abstract: 170 words

22   Text (excluding references and figure legends): 4609

23

Abstract:

We have developed a transencapsidated vaccine delivery system based on the insect virus, *Flock House virus* (FHV). FHV is attractive due to its small genome size, simple organization, and non-pathogenic characteristics. With the insertion of a *Tobacco mosaic virus* (TMV) origin of assembly (Oa), the independently replicating FHV RNA1 can be transencapsidated by TMV coat protein. In this study we demonstrated that the Oa adapted FHV RNA1 transencapsidation process can take place *in planta*, by using a bipartite plant expression vector system, where TMV coat protein is expressed by another plant virus vector, *Foxtail mosaic virus* (FoMV). Dual infection in the same cell by both FHV and FoMV was observed. Though an apparent classical coat-protein-mediated resistance repressed FHV expression, this was overcome by delaying inoculation of the TMV coat protein vector by three days after FHV vector inoculation. Expression of transgene marker in animals by these *in vivo* generated transencapsidated nanoparticles was confirmed by mouse vaccination, which also showed an improved vaccine response compared to similar *in vitro* produced vaccines.

Introduction

Virus-based nanoparticles have been extensively explored as a vaccine delivery strategy due to their typically higher immunogenicity compared with unassembled vaccine antigens (1, 2), their potential to serve as their own adjuvant (1-3), and their greater safety and potentially relatively lower cost of protection compared to traditional vaccines(4). Virus-like particles (VLPs) display vaccine antigen on their surface and can be produced by the self-assembly of viral coat protein subunits expressed in a heterologous host, such as bacteria (5) or plants (6), or in mammalian cells (7). An alternative to VLPs is to use viral coat protein to encapsidate the RNA of another virus, with the RNA expressing the vaccine antigen once delivered to the target cell. In this way, the viral RNA can be packaged in an especially resistant nanoparticle similar to a VLP. The potential advantage of this strategy over VLPs is the activation of innate immunity by viral replication (8-10).

Among numerous trials using viral nanoparticles for antigen delivery, *Tobacco mosaic virus* (TMV) nanoparticles seem to hold special promise. TMV virions are characterized by great stability and low cost production (11), and a recent study suggests that the human population has already been extensively exposed to TMV coat antigen through exposure to food and tobacco sources (12). Furthermore, extensive data show that pre-existing immunity to TMV coat does not disrupt boosting of either cytotoxic T lymphocyte (CTL, (13, 14)

68 or antibody target antigens (15, 16). Lastly, TMV virions are extremely stable,

69 remaining infective for over a century at room temperature (17). TMV exhibits

70 robust expression in plants at up to 5-10% dry weight, and is easy to purify at

71 the commercial scale (11).

72

73 Consequently, TMV nanoparticles have been explored as a VLP epitope

74 platform. The highly uniform repeated organization of 2130 copies of coat

75 protein subunits and the associated strong cross-linking pattern provide

76 greatly improved efficacy to deliver antigens to antigen presenting cells.

77 Various studies have validated that TMV-antigen conjugation can induce B

78 cell activation and raised antibody titers (15, 18, 19), even when the

79 conjugates are poorly immunogenic, such as carbohydrates (20).

80 Furthermore, TMV uptake by dendritic cells is rapid and efficient (14, 18), and

81 peptide-presenting TMV nanoparticles were proven to be able to elicit T cell

82 responses with augmented interferon gamma (IFNγ) levels (14). We have

83 also previously successfully tested ovalbumin-conjugated TMV vaccines, as

84 well as a bivalent TMV vaccine displaying both mouse melanoma-associated

85 CTL epitopes p15e and tyrosinase-related protein 2 (Trp2) peptides (13).

86 Immunization resulted in a significantly improved survival after lethal tumor

87 challenge. A recent study also demonstrated TMV's great potential to be used

88 in stand-alone or prime-boost dendritic cell activation strategies (18).

89

90   In addition to utilizing TMV as a VLP to present surface epitopes,

91   development has also proceeded with TMV coat protein encapsidated RNA

92   vaccines. In previous experiments, we have produced and tested Semliki

93   Forest virus (SFV) RNA encapsidated with TMV coat protein *in vitro*.

94   Attenuated SFV was modified by insertion of a TMV origin of assembly to

95   produce, *in vitro*, rod shaped virus particles that resembled TMV (21) by

96   mixing SFV-Oa RNA with purified TMV coat protein. Vaccination with SFV-Oa

97   encoding the model antigen beta-galactosidase (bGal) resulted in boosted

98   antibody responses to bGal protein, demonstrating that TMV encapsidated

99   RNA was translated and was antigenic in the absence of adjuvant, and,

100   further, that the presence of the TMV Oa did not disrupt SFV replication

101   functions. However, as a common phenomenon of pathogenic RNA virus

102   vaccines (22), SFV-Oa RNA induced apoptosis in infected cells, which may

103   limit duration of antigen exposure and reduce immune activation to transgene

104   encoded antigens.

105

106   To improve on our previous results with SFV, we applied TMV encapsidation

107   to the RNA of the nonpathogenic insect virus, *Flock House virus* (FHV), which

108   is capable of replicating in human cells. The advantages of FHV include a

109   bipartite genome, where the polymerase is encoded by the independently

110   replicating RNA 1 and the structural capsid gene is encoded by RNA 2,

111   allowing for easy manipulation of the RNA1 genome for vaccine development

112 and the separation of replication from packaging. We have already tested *in*

113 *vitro* assembled TMV-FHV particles and have shown that TMV Oa did not

114 disrupt FHV viral replication, using an enhanced green fluorescent protein

115 (eGFP) transgene to monitor replication and expression in mammalian cells

116 (23). However, the limitations of *in vitro* encapsidation remain with this

117 system; namely the cost of RNA synthesis and potentially reduced translation

118 due to inefficient *in vitro* 5' capping.

119

120 To overcome these limitations, we explored an *in planta* strategy for

121 producing viral RNA *in vivo*. For the present study, we hypothesized that FHV

122 RNA, which replicates well in mammalian (24) and plant cells (25) but is not a

123 pathogen of either, could be encapsidated *in planta* if sufficient TMV coat

124 protein were provided *in trans*. We further predicted that *in planta* produced

125 nanoparticles would be able to express transgene after animal vaccination,

126 and will be comparatively more immunogenic than *in vitro* nanoparticles due

127 to natural 5' capping. As described in the following report, we used a 35S

128 promoter to express FHV-eGFP-Oa RNA and the plant viral vector Foxtail

129 mosaic virus (FoMV) to express TMV coat protein in quantities sufficient for

130 encapsidation of FHV RNA in agroinoculated *Nicotiana benthamiana* plants.

131 Replication of functional FHV-eGFP-Oa was observed as an unusually strong

132 eGFP fluorescence, and near wild type levels of TMV-coat protein were

133 produced by co-delivered FoMV vector. We observed virion particles of the

134   typical TMV morphology as a final product. When these nanoparticles were

135   used to vaccinate mice, the expression of eGFP transgene was confirmed by

136   an anti-eGFP immune response greater than that observed for *in vitro*

137   encapsidated control particles. This is the first report of *in planta*

138   transencapsidated nanoparticles and represents the first step towards

139   producing a commercially viable vaccine of this type.

140

141   **MATERIALS AND METHODS**

142   **Construction of T7/FHV-C2-GFP vector and expression in mammalian**

143   **cells.** The plasmid containing the FHV RNA1 expression cassette was kindly

144   provided by Dr. A. Ball. It is a T7 promoter-driven plasmid containing the

145   RNA1 portion of the FHV genome and was previously described (26). A

146   polylinker, CTCGAGGCGATCGCCTGCAG, encompassing the 3 restriction

147   sites XhoI, AsiSI and PstI, was cloned into one of four insertion sites: C1, nt.

148   3034; C2, nt. 3037; C3, nt. 2731; and C4, nt. 3055, and confirmed by direct

149   sequencing. Enhanced green fluorescent protein (eGFP) ORF was then

150   cloned into these sites via XhoI and PstI to create T7/FHV-C-(1-4)-GFP

151   constructs (Fig. 1A). To confirm stability of the eGFP modified FHV viral RNA,

152   full-length RNA transcripts were generated from the T7/FHV-C-GFP DNA *in*

153   *vitro* via a T7 promoter kit (mMESSAGE mMACHINETM, Ambion, TX). 2 μg

154   RNA was used to transfect BHK-21 cells with DMRIE-C (Invitrogen, Carlsbad,

155   CA). Transfected cells were incubated at 37°C for 4 hours, after which fresh

156   growth media was used to replace transfection media. Cells were then placed

157   at 28°C for 24 hours. Expression of fluorescence was confirmed using a

158   Nikon Eclipse TS100 microscope and NIS-elements imaging software. Cells

159   were observed for 2 days post-transfection.

160

161   ***In planta* expression vectors.** In order to express FHV in plants, full-length

162   FHV viral vector sequence was transferred from T7/FHV-C2-GFP (Fig. 1A)

163   and placed between the StuI/XbaI sites of the plant binary vector JL22 (27) to

164   create 35S/FHV-C2 (Fig. 2A). To allow Oa insertion, additional restriction

165   sites were introduced on either side of the eGFP ORF by amplifying the eGFP

166   ORF with an upstream primer containing XhoI/AscI and a downstream primer

167   containing AvrII/PstI and then reinserting this product into 35S/FHV-C2

168   between the XhoI and PstI sites. TMV Oa (95 bp: TMV nts. 5432-5527; (28)

169   was inserted upstream or downstream of the eGFP ORF to create

170   35S/FHVC2-o1 and -o2, respectively (Fig. 2A). PCR with a primer containing

171   a mutated eGFP ORF stop codon was used to create 35S/FHVC2-o3.

172

173   Several modifications were made to improve eGFP expression. T7/FHV-C4-

174   2sg was created to maintain B2 expression, by duplicating the 3' end of FHV

175   RNA1 (nt. 2518-3055) and inserting it after the eGFP open reading frame in

176   T7/FHV-C4-GFP. 35S/FHV-C4-2sg (Fig. 2B) was generated by transferring

177   the viral sequence into JL22 (27), as outlined above. To express both FHV B2

178 and eGFP separately, a 498 bp DNA segment was synthesized (gBlock, IDT,

179 Coralville, IA) and inserted between the XhoI and PstI sites in 35S/FHV-C4.

180 This segment contained a stop codon in the B2 ORF, 10 bp of the FHV 3'

181 UTR for any potential required context for B2 ORF expression, the 95 bp TMV

182 Oa, a repeat of the presumed B2 subgenomic promoter (FHV 2480-2809,

183 including 69 bp past the B2 start) to drive eGFP expression, and a start codon

184 and insertion sites for eGFP. To recreate a more FHV authentic 3' region

185 following the eGFP ORF, the final 24 bases of B2 ORF was added

186 downstream of the eGFP stop codon, to yield the final construct:

187 35S/FHV2sg2 (Fig. 2B). All recombinant DNA methods and suppliers for the

188 plant constructs were as previously described (29).

189

190 **Agroinoculation and visualization.** *Nicotiana benthamiana* plants were

191 grown and agroinoculated as previously described (29). Excised eGFP-

192 fluorescent leaves were visualized using a blue light Dark Reader (Clare

193 Chemical, Dolores, CO, USA). The defective interfering construct

194 DI638/wtGFP (30) was a gift from A. Rao (UC Riverside) and those

195 inoculations were visualized with a hand held UVL-56 lamp (UVProducts,

196 Upland, CA, USA).

197

198 Relative fluorescence resulted by different FHV constructs was measure by

199 grinding inoculated leaf tissue in 1X Phosphate Buffered Saline (PBS). The

200 collected supernatant was assessed on a microplate reader (Thermo

201 Fluoroskan Ascent FL), with black 96 well plate (COSTAR 3925, Corning Inc.

202 NY). Filter set of 485nm (excitation) and 538nm (emission) was used in order

203 to detect eGFP fluorescence.

204

205 **Plant protoplasts.** Protoplasts were prepared from *N. benthamiana* leaves 4

206 days post-inoculation. Leaves were sliced into 2 mm strips and vacuum

207 infiltrated with MMC buffer (13% mannitol, 5 mM MES, 10 mM $CaCl_2$, pH 5.8)

208 containing 1% Onozuka cellulase RS and 0.5% Macerase (both from

209 Phytotechnology Labs, Shawnee Mission, KS, USA) and gently rocked

210 overnight. Protoplasts were mounted in MMC on a glass slide. Images were

211 obtained as previously described (29).

212

213 **Plant produced nanoparticles.** To purify nanoparticles, agroinoculated *N.*

214 *benthamiana* leaves, 4-7 days p.i., were ground in a mortar in extraction

215 buffer (50 mM sodium acetate, 0.86 M NaCl (5% w/v), 0.04% sodium

216 metabisulfite, pH 5.0). Crude homogenate was filtered through cheesecloth

217 and 8% (v/v) n-butanol was added, and then incubated at room temperature

218 for 15 min, and then centrifuged at 10,000 x g for 15 min. The supernatant

219 was decanted through cheesecloth, and nanoparticles were precipitated with

220 PEG 8000 (EMD Millipore, USA) at 4% on ice for 1 hr, followed by

221 centrifugation at 10,000 x g for 10 min. The pellet was resuspended in a

222   minimum of 10 mM phosphate buffer (pH 7.2) and then centrifuged at 16,000

223   x g for 10 min. The supernatant was collected and nanoparticles were purified

224   with an additional round of PEG precipitation. The final nanoparticle pellet

225   was suspended in 10mM phosphate buffer (pH 7.2) and stored at -20°C.

226   Protein concentration was determined by bicinchoninic acid (BCA) assay

227   (Pierce Biotechnology, Rockford, IL, USA).

228

229   Transmission electron microscopy was used to visualize purified

230   nanoparticles on a JEOL JSM 1010 microscope. A 3 µl drop of nanoparticles

231   was adsorbed onto 300 mesh formvar coated grids (Electron Microscopy

232   Sciences, PA, USA) for 1 minute, drawn off, and stained with 1%

233   phosphotunstic acid (pH 7). Image was taken by XR16 TEM camera

234   (Advanced Microscopy Techniques, MA, USA), and with AMT Image Capture

235   Engine V602 (Advanced Microscopy Techniques, MA, USA), at 30,000X to

236   40,000X magnification.

237

238   ***In vitro* nanoparticle assembly and vaccine preparation.** SFV-eGFP or

239   FHV-eGFP RNA was transcribed from T7 plasmids using a capped RNA

240   synthesis kit (MmessageMachine; Ambion), quantitated by absorbance, and

241   checked for integrity by gel electrophoresis. 50 µg of RNA was then incubated

242   with 1.4 mg of TMV coat protein, prepared by a modified protocol as

243   previously described (21). Briefly, encapsidations were carried out using

244   overnight incubation in a 0.05 M phosphate buffer (pH7) at room temperature.

245   Particles were recovered by PEG precipitation and quantitated by BCA assay

246   (BioRad, CA).

247

248   **Vaccination and immune response evaluation in mice.** BALB/c mice

249   (Charles River, CA) were housed at Touro University according to guidelines

250   established in the Care and Use of Animals, and performed according to

251   IACUC approved protocols. Typically, 3 mice were given a 100 – 200 µl

252   subcutaneuous (s.c.) injection of 15 or 30 µg encapsidated product, or 15 µg

253   eGFP protein as a positive control (Vector Labs), or PBS as a negative

254   control. Vaccines were typically administered at two-week intervals and tail

255   vein bleeds were taken at 10 days after vaccines 2 and 3 for enzyme linked

256   immunosorbent assay (ELISA) analysis.

257

258   The IgG immune response was determined by ELISA. 96-well microtiter

259   plates (MaxiSorp; Nalge Nunc) were coated with 5 µg/ml eGFP protein

260   (Vector Labs) in 50 mM carbonate/bicarbonate buffer (pH 9.6). After blocking

261   with 2% bovine serum albumin (BSA) in PBS, serial dilutions of the sera were

262   added for one hour, the plates were washed and incubated for an additional

263   hour with anti-mouse IgG Horse Radish Peroxidase (HRP) conjugated

264   secondary antibody (Southern Biotech) in PBS+BSA. Plates were developed

265   using a tetramethyl benzidine substrate solution (TMB; BioFx) and the

266 reactions were stopped by the addition of 1N sulfuric acid. Plate absorbance

267 was read at 450 nm in a 96-well plate spectrophotometer (Molecular

268 Devices). Relative anti-eGFP titers reported were determined from a standard

269 curve generated by a 3-fold serial dilution of a 100 ng/ml rabbit anti-eGFP

270 polyclonal antibody (Sigma) detected with an anti-Rabbit-HRP secondary.

271 Statistical analysis was carried out using Prism software (GraphPad), using

272 unpaired t-test with Welch's correction.

273

274 **RESULTS**

275 **FHV vector expression in mammalian cells.** FHV vectors were designed

276 and tested for the expression of eGFP in BHK-21 cells. A cassette containing

277 three restriction sites (XhoI, AsiI and PstI) was placed at the FHV C2 site (31);

278 namely, immediately downstream of the polymerase/B1 stop codon, which is

279 also six codons upstream from, and in phase with, the B2 stop codon (Fig.

280 1A). This FHV-C2 construct thus expresses a B2-eGFP-B2 fusion, with 99

281 amino acids of B2 upstream of eGFP and 6 amino acids of B2 at the C

282 terminus. Insertion at a second eGFP ORF insertion site, the C4 site, would

283 produce the full B2 protein fused to the eGFP (Fig. 1A). eGFP expression

284 was observed in mammalian cells (Fig. 1B) within 24 hours post transfection.

285 Expression with both constructs peaked at 48 hours and was maintained until

286 72 hours, with approximately 15-20% transfection efficiency. Fluorescence

287 began to decrease after 72 hours and gradually diminished over time. The C4

288 insertion construct gave reduced fluorescence compared to C2 (Fig. 1B).

289

290 **Strong FHV/eGFP expression in *N. benthamiana* after p19 co-**

291 **agroinoculation.** The 35S/FHV-C2-GFP and 35S/FHV-C4-2sg constructs

292 were made by transferring viral sequences from the mammalian vectors into

293 plant binary vector pJL22 (27) between a cauliflower mosaic virus 35S

294 promoter and 35S terminator (Fig. 2). Leaves agroinoculated with these

295 constructs gave a weak fluorescence (Fig. 3), as did leaves inoculated with

296 the positive FHV/wtGFP control, F1DI, comprising FHV RNA1 and DI638, the

297 defective interfering RNA of FHV RNA2, carrying wtGFP (30). However, when

298 the silencing suppressor, p19 (32), was provided by co-agroinoculation, a

299 much stronger fluorescence was observed (Fig. 3) which was much stronger

300 than the F1DI + p19 control. Subsequently, p19 was included in all

301 inoculations.

302

303 To create a FHV vector competent for encapsidation by TMV CP, the TMV

304 Oa was inserted into 35S/FHV-C2-GFP at two different positions (35S/FHV-

305 C2-o1, o2), and adjacent to eGFP ORF. In order to test the influence of C

306 terminal TMV Oa fusion on eGFP expression, a third construct, 35S/FHV-C2-

307 o3, was designed with the introduction of a stop codon at the natural stop site

308 of eGFP, resulting in an eGFP fusion with B2 only at the N terminus. These

309   three Oa containing constructs (35S/FHV-C2-o1 to o3) were found to express

310   only slightly less eGFP in leaves than the non-Oa, 35S/FHV-C2 (Fig. 3 and

311   Fig. 4A). This was unexpected since the TMV Oa sequence was added close

312   to either the putative sub-genomic promoter or the FHV 3'UTR. Little

313   difference in fluorescence was observed between the three Oa containing

314   constructs.

315

316   To express the FHV silencing suppressor, B2 (Albariño et al., 2003), in

317   conjunction with eGFP, we made variants of 35S/FHV-C4-2sg. To prevent the

318   deletion of the eGFP ORF, we placed the eGFP ORF at the 3' terminus of the

319   virus, in contrast to the C4-2sg construct. Any homologous recombination

320   between the two homologous subgenomic regions would delete B2 and Oa,

321   but not eGFP, and deletion mutants would not be packaged as nanoparticles.

322   It was observed that the 35S/FHV-C2-GFP construct clearly resulted in a

323   brighter fluorescence than 35S/FHV-C4-2sg, which was further confirmed by

324   fluorometry analysis (Fig. 4A).

325

326   To explore the impact of improved B2 expression, a portion of the FHV 3'

327   UTR, which is normally downstream of the B2 ORF, was added to the internal

328   B2 ORF followed by the TMV Oa. The final construct 35S/FHV2sg2 was

329   created by adding 24 bp of C-terminal B2 sequence to aid eGFP expression

330   by providing more natural context at the 3' end of the ORF. We expected to

331   see stronger eGFP expression and/or FHV B2 expression that would

332   functionally replace p19. However, the FHV2sg2 vector did not significantly

333   improve eGFP fluorescence expression compared with the original C4-2sg

334   construct *in planta* (Fig. 3). Other constructs were built and tested, which

335   included the precedent construct of FHV2sg2 (data not included) and a vector

336   with the addition of strong Kozak context in pursuit of enhanced expression

337   (FHV2sg2KSS, supplementary Fig 1a). Neither resulted any improvement in

338   eGFP fluorescence (Fig 3). In all cases, p19 was still required via co-

339   agroinoculation for strong fluorescence. All subsequent experiments used the

340   35S/FHV-C2-o3 construct co-agroinoculated with p19.

341

342   **Co-expression of FHV and FECT in plants**

343   To encapsidate FHV vector RNA *in planta*, a ratio of 20:1 mass ratio of TMV

344   coat protein (CP) to RNA is required. The high expression *Foxtail mosaic*

345   *virus* vector, FECT (29), was used to produce TMV CP without being itself

346   encapsidated. FECT produced TMV CP at a level comparable to the TMV

347   vector JL24 (27), which expresses TMV CP as a native gene (Fig. 5).

348

349   We next examined the ability of FHV and FECT to co-infect cells, to ensure

350   there was no replication interference. In a co-infection test system, 35S/FHV-

351   C2 expressing eGFP and FECT expressing DsRed were co-agroinoculated

352   into several leaves, resulting in a yellow-green fluorescence under blue light

353   when viewed without magnification (Fig. 6A). In order to determine co-

354   infection of single cells, co-infected leaves were reduced to protoplasts and

355   the protoplasts were examined under a UV microscope. As seen in a

356   representative photo (Fig. 6B), about 75% of the eGFP positive cells are also

357   DsRed positive, but not vice versa. FECT strongly infects the great majority of

358   plant cells (29), as seen by the DsRed signals in Fig. 6B. FHV/eGFP is an

359   insect virus construct and infects a much smaller number of plant cells, but

360   those that are infected are mostly co-infected with FECT/DsRed,

361   demonstrating the high frequency at which double infection occurs with this

362   system, given the limitations of FHV infectivity itself.

363

364   **eGFP expression by FHV enhanced by delayed TMV CP expression**

365   Nanoparticles were produced by agro-inoculation with 35S/p19, 35S/ FHV-

366   C2-o3, and 35S/FECT-TMVCP. The average size of our FHV-C2-o3

367   nanoparticles is estimated to be ~200nM based on the length of the FHV RNA

368   genome (C2-o3; 4182 nts.), compared with wide type TMV (6395 nts.) that

369   generates a 300nM particle (Fig. 7).

370

371   In all experiments, the presence of TMV CP at the time of FHV early infection

372   (i.e., co-inoculation) led to reduced eGFP fluorescence. We hypothesized that

373   CP binding the Oa early in infection impeded the replicative or translational

374   events of FHV RNA. To test this, a "2-step" protocol was used in which the

375   FECT/TMV CP inoculation was delivered three days after the FHV/GFP/Oa

376   and p19 inoculations. The 2-step procedure consistently increased eGFP

377   expression (Fig. 4).

378

379   **Immune response to nanoparticles in mice**

380   In order to test the capacity of transencapsidated FHV RNA to express the

381   eGFP transgene in mice, *in planta* transencapsidated FHV RNA was used to

382   immunize BALB/c mice with *in vitro* transencapsidated FHV RNA or SFV RNA

383   as encapsidation controls. Two doses of 15 µg or 30 µg encapsidated RNA

384   (0.75 or 1.5 µg of RNA, respectively) were given by subcutaneous injection,

385   without adjuvant. eGFP protein (15 µg) was used as a positive control while

386   PBS buffer was used as a negative control. Sera collected from mice before

387   immunization and after a single dose were essentially negative for immune

388   responses for all groups (data not shown). Weak but detectable anti-eGFP

389   IgG responses were measured by ELISA after a second vaccination (pV2,

390   Fig. 8), but all groups were statistically similar to PBS, including eGFP protein

391   immunization. After a third immunization (pV3), all groups showed a strong

392   trend toward augmented immunity against eGFP, but in large part were not

393   significantly different than PBS, mainly due to high variance between

394   responders and small group size. However, the highest dose of *in planta*

395   encapsidated FHV (C2-o3, 30µg) and eGFP protein control had IgG titers

396   significantly higher than all *in vitro* encapsidated viral vector treatments. This

397   confirmed the successful expression of eGFP transgene by

398   transencapsidated FHV RNA, after uptake and presumed co-translational

399   disassembly of TMV coat protein. This is notable, in light of low replication

400   ability of FHV RdRp in animal cells at 37 degree (33).

401

402   **Discussion**

403   We have shown in this study that FHV can be encapsidated *in planta* with

404   TMV coat protein and the resulting nanoparticle vaccines had improved

405   characteristics compared to *in vitro* encapsidated FHV RNA. In previous

406   studies, we demonstrated that SFV could be encapsidated *in vitro* with TMV

407   coat protein (21). TMV coat protein produced *in vivo* had also been used to

408   assemble wild type TMV virions in *E. coli* (34) and mRNAs had been

409   encapsidated *in planta* to form TMV hybrid virions (35). As well, *Brome*

410   *mosaic virus* (BMV) RNA containing the TMV Oa was transencapsidated with

411   TMV CP in barley protoplasts (36) and Rao and colleagues produced non-

412   specific transencapsidated virions by coat protein of the similarly structured

413   BMV in studying encapsidation specificity (37). Though FHV virions use a

414   multitude of molecular cues in virion assembly, similar to other icosahedral

415   viruses (38), TMV and other tobamoviruses utilize a single Oa sequence to

416   initiate assembly, with the remainder of the encapsidated sequence

417   apparently without further molecular cues (39). Thus, any RNA containing the

418   TMV Oa should be able to be transencapsidated. It may be possible to extend

419 this technique to other viral species for viral-vectored nanoparticle vaccine

420 assembly *in planta*.

421

422 The individual components of the nanoparticles appeared to be produced at

423 high levels. The FECT viral vector produced TMV CP at the same level as the

424 native TMV vector, JL24(Fig 5). FHV vector levels, as measured by visually

425 assessed fluorescence of eGFP (Fig. 3), were greater in side by side studies

426 than the DI638 vector used in previous FHV work in *N. benthamiana* (37).

427 The coexpression of p19 silencing suppressor further boosted this eGFP

428 expression even with FHV vector constructs that had an intact B2 silencing

429 suppressor (Fig.2 and 3).

430

431 As a prerequisite for assembly, coexpression of both vectors in a single cell is

432 necessary. The FECT vector was shown to express in the majority of cells

433 harboring the FHV vector (Fig. 6). However, when FHV RNA and TMV CP

434 vectors were co-inoculated, we saw a significant decrease in fluorescence. A

435 supplementary experiment was performed in order to exclude the possibility

436 of FECT interfering FHV replication (suppl. Fig. 2). This inhibition

437 phenomenon is most likely mediated by classical coat protein resistance (40)

438 and was previously observed by the Ahlquist group working with BMV

439 transencapsidated by TMV CP. BMV RNAs 1 and 2 containing the TMV Oa

440 decreased in replication 20-fold when co-inoculated with BMV RNA 3

441   expressing TMV CP (36). This was theorized to be due to TMV CP binding to

442   the BMV RNAs and interfering with replication. We investigated this

443   hypothesis by separating the agroinoculation of FHV vector and TMV CP into

444   two steps, delaying the expression of TMV CP until FHV RNA replication was

445   sufficient to generate robust eGFP protein. The two-step plants consistently

446   showed higher expression of the viral eGFP transgene (Fig. 4), suggesting

447   RNA packaging by TMV CP reduced FHV RNA replication and/or translation.

448

449   Several modifications were made in an attempt to improve FHV vector

450   replication in plants. The addition of TMV Oa led to strong inhibition of BMV

451   RNA replication even in the absence of TMV CP in a previous study (36).

452   However, we observed only a slight decrease in eGFP production by the FHV

453   vectors carrying Oa. C2 constructs carrying Oa at two different sites (C2-o1

454   and C2-o2) did not differ significantly in eGFP fluorescence produced.

455   Recreating a native C-terminus for eGFP (C2-o3) also had no effect.

456   Constructs with unmodified B2 silencing suppressor ORFs (2sg2 series) were

457   less effective than the C2 series with the B2 ORF fused to eGFP. These were

458   longer constructs, but the shorter C4 construct was also less fluorescent in

459   mammalian cells than the C2 construct (Fig. 1B), suggesting the common C4

460   insertion site as detrimental. Ultimately, the inclusion of p19 as a co-inoculant

461   was the sole factor in achieving high eGFP expression in plants from the FHV

462   vectors, re-confirming the importance of mitigating RNA silencing *in planta*.

463

464   It is possible that the size of the duplicated subgenomic promoter in the 2sg2

465   series was insufficient since a longer FHV subgenomic promoter segment

466   was found more efficacious in a previous study (41). Beyond the core nts.

467   2518-2777, the region from nt. 2302-2518 may serve as an important

468   enhancer (42). Polarity preference was found on FHV (41) and other positive-

469   strand RNA viruses; specifically, that two pieces of sgRNA were replicated at

470   different levels, with the longer one (closer to replicase) being dominant. This

471   may explain why we see more eGFP fluorescence in the 35S/ FHV-C4-2sg,

472   which has the eGFP ORF included in the first sgRNA3, than–FHV-2sg2

473   series, which have eGFP ORF included in the second sgRNA3.

474

475   In order to verify the capacity of these transencapsidated nanoparticles to

476   express transgene in animal cells, FHV C2-o3 encapsidated particles were

477   used as a vaccine, and an IgG antibody response to eGFP was measured

478   (Fig. 8). Despite the reported deficiency of FHV replicase to function well in

479   37 degree (33), a titer of anti-eGFP antibody equal to that of 15ug eGFP

480   protein was observed after three injections with 30 ug of FHV C2-o3

481   nanoparticles (1.5ug FHV RNA). This demonstrated delivery and expression

482   of the eGFP transgene and suggested a considerable boosting of the immune

483   response by RNA antigen delivery. *In vitro* FHV and SFV/TMV CP

484   nanoparticles produced a significantly lower immune response in this study,

485   possibly due to lower percentage of 5' capping, which is known to affect

486   translation efficiency.

487

488   During nanoparticle *in planta* assembly, FHV subgenomic RNA3 may also be

489   encapsidated by TMV coat proteins, co-purified and be represented in mice

490   injections. The possibility of sgRNA3 being used as mRNA templates has

491   been considered, since sgRNA3 also contains eGFP sequence and contains

492   a TMV 0a. However, from the numerous TEM images, it is apparent that the

493   amount of sgRNA3 nanoparticles (~67nM) is not evident or a minority of the

494   particles, and the majority nanoparticles are of full length (200nm) .

495   Furthermore, from the previous literature, the non-replicating mRNA

496   vaccination strategy has largely relied on extensive chemical modifications,

497   additional use of adjuvants (43), and an *ex vivo* route to transinfect dendritic

498   cells(44). In two studies using eGFP mRNA to transinfect dendritic cells,

499   eGFP either degraded too rapidly due to the lack of additional targeting

500   signals(46), or was expressed well in dendritic cells but failed to trigger

501   dendritic cell maturation without using inducing agents(47). Overall, it is more

502   likely that a functional replicase and a self-replicating viral RNA account for

503   the bulk of the immune stimulation observed in this work, rather than

504   translation from sgRNA3.

505

506 Several improvements can be made to the utility of TMV coat encapsidated

507 RNA. In order to increase immune activation and greater CD4 T cell

508 response, future optimization may include the use of other viruses with a

509 replicase active at 37 degree, such as Nodamura virus (33). Peptide directed

510 endosomal escape of nanoparticles (48-50) may also increase animal cell co-

511 translational disassembly, and subsequent protein accumulation. In our study,

512 eGFP was used to track viral expression of eGFP in plant and animal cells.

513 Expression of a more potent immunogen (e.g., ovalbumin) with better

514 characterized antigenicity should also improve measurement of both antibody

515 and T cell immunogenicity after nanoparticle vaccination.

516

517 In conclusion, we were able to produce FHV RNA and TMV CP, in the same

518 plant cell, resulting in assembly of rod shaped packaged RNA. These *in*

519 *planta* produced nanoparticles were shown to induce an antigen-specific

520 immunogenicity exceeding that of *in vitro* packaged RNA nanoparticles. Our

521 next tasks are to investigate cellular localization of FHV RNA and TMV CP

522 and to optimize heterologous virion assembly. We will also seek to target the

523 hybrid virion nanoparticles to the correct compartment in the mammalian cell

524 in order to facilitate TMV-CP virion disassembly and improved RNA 1

525 replication. Completion of these goals will answer basic virological questions

526 of component trafficking, disassembly and replication in the process of

527 optimizing vaccine production and potency.

528

529

530

531

532

533

References

535   1. Gutierro, I., Hernandez, R. M., Igartua, M., Gascon, A. R. and Pedraz, J. L. (2002)
536   Influence of dose and immunization route on the serum Ig G antibody response
537   to BSA loaded PLGA microspheres. Vaccine 20, 2181-2190.
538   2. Gutierro, I., Hernandez, R. M., Igartua, M., Gascon, A. R. and Pedraz, J. L. (2002)
539   Size dependent immune response after subcutaneous, oral and intranasal
540   administration of BSA loaded nanospheres. Vaccine 21, 67-77.
541   3. Dobrovolskaia, M. A. and McNeil, S. E. (2007) Immunological properties of
542   engineered nanomaterials. Nature nanotechnology 2, 469-478.
543   4. McCormick, A. A., Reddy, S., Reinl, S. J., Cameron, T. I., Czerwinkski, D. K.,
544   Vojdani, F., Hanley, K. M., Garger, S. J., White, E. L., Novak, J., Barrett, J., Holtz, R. B.,
545   Tuse, D. and Levy, R. (2008) Plant-produced idiotype vaccines for the treatment
546   of non-Hodgkin's lymphoma: safety and immunogenicity in a phase I clinical
547   study. Proceedings of the National Academy of Sciences of the United States of
548   America 105, 10131-10136.
549   5. Aires, K. A., Cianciarullo, A. M., Carneiro, S. M., Villa, L. L., Boccardo, E., Perez-
550   Martinez, G., Perez-Arellano, I., Oliveira, M. L. and Ho, P. L. (2006) Production of
551   human papillomavirus type 16 L1 virus-like particles by recombinant
552   Lactobacillus casei cells. Applied and environmental microbiology 72, 745-752.
553   6. Huang, Z., Santi, L., LePore, K., Kilbourne, J., Arntzen, C. J. and Mason, H. S.
554   (2006) Rapid, high-level production of hepatitis B core antigen in plant leaf and
555   its immunogenicity in mice. Vaccine 24, 2506-2513.
556   7. Zhou, J., Sun, X. Y., Stenzel, D. J. and Frazer, I. H. (1991) Expression of vaccinia
557   recombinant HPV 16 L1 and L2 ORF proteins in epithelial cells is sufficient for
558   assembly of HPV virion-like particles. Virology 185, 251-257.
559   8. Diebold, S. S., Kaisho, T., Hemmi, H., Akira, S. and Reis e Sousa, C. (2004) Innate
560   antiviral responses by means of TLR7-mediated recognition of single-stranded
561   RNA. Science 303, 1529-1531.
562   9. Lund, J. M., Alexopoulou, L., Sato, A., Karow, M., Adams, N. C., Gale, N. W.,
563   Iwasaki, A. and Flavell, R. A. (2004) Recognition of single-stranded RNA viruses

564   by Toll-like receptor 7. Proceedings of the National Academy of Sciences of the
565   United States of America 101, 5598-5603.
566   10. Schwarz, K., Storni, T., Manolova, V., Didierlaurent, A., Sirard, J. C.,
567   Rothlisberger, P. and Bachmann, M. F. (2003) Role of Toll-like receptors in
568   costimulating cytotoxic T cell responses. European journal of immunology 33,
569   1465-1470.
570   11. Pogue, G. P., Lindbo, J. A., Garger, S. J. and Fitzmaurice, W. P. (2002) Making
571   an ally from an enemy: plant virology and the new agriculture. Annual review of
572   phytopathology 40, 45-74.
573   12. Liu, R., Vaishnav, R. A., Roberts, A. M. and Friedland, R. P. (2013) Humans
574   have antibodies against a plant virus: evidence from tobacco mosaic virus. PloS
575   one 8, e60621.
576   13. McCormick, A. A., Corbo, T. A., Wykoff-Clary, S., Palmer, K. E. and Pogue, G. P.
577   (2006) Chemical conjugate TMV-peptide bivalent fusion vaccines improve
578   cellular immunity and tumor protection. Bioconjugate chemistry 17, 1330-1338.
579   14. McCormick, A. A., Corbo, T. A., Wykoff-Clary, S., Nguyen, L. V., Smith, M. L.,
580   Palmer, K. E. and Pogue, G. P. (2006) TMV-peptide fusion vaccines induce cell-
581   mediated immune responses and tumor protection in two murine models.
582   Vaccine 24, 6414-6423.
583   15. Smith, M. L., Lindbo, J. A., Dillard-Telm, S., Brosio, P. M., Lasnik, A. B.,
584   McCormick, A. A., Nguyen, L. V. and Palmer, K. E. (2006) Modified tobacco mosaic
585   virus particles as scaffolds for display of protein antigens for vaccine
586   applications. Virology 348, 475-488.
587   16. Mallajosyula, J. K., Hiatt, E., Hume, S., Johnson, A., Jeevan, T., Chikwamba, R.,
588   Pogue, G. P., Bratcher, B., Haydon, H., Webby, R. J. and McCormick, A. A. (2013)
589   Single-dose monomeric HA subunit vaccine generates full protection from
590   influenza challenge. Human vaccines & immunotherapeutics 10, 586 - 595.
591   17. Fraile, A., Escriu, F., Aranda, M. A., Malpica, J. M., Gibbs, A. J. and Garcia-Arenal,
592   F. (1997) A century of tobamovirus evolution in an Australian population of
593   Nicotiana glauca. Journal of virology 71, 8316-8320.
594   18. Kemnade, J. O., Seethammagari, M., Collinson-Pautz, M., Kaur, H., Spencer, D.
595   M. and McCormick, A. A. (2014) Tobacco mosaic virus efficiently targets DC
596   uptake, activation and antigen-specific T cell responses in vivo. Vaccine 32,
597   4228-4233.
598   19. Koo, M., Bendahmane, M., Lettieri, G. A., Paoletti, A. D., Lane, T. E., Fitchen, J.
599   H., Buchmeier, M. J. and Beachy, R. N. (1999) Protective immunity against murine
600   hepatitis virus (MHV) induced by intranasal or subcutaneous administration of
601   hybrids of tobacco mosaic virus that carries an MHV epitope. Proceedings of the
602   National Academy of Sciences of the United States of America 96, 7774-7779.
603   20. Yin, Z., Nguyen, H. G., Chowdhury, S., Bentley, P., Bruckman, M. A., Miermont,
604   A., Gildersleeve, J. C., Wang, Q. and Huang, X. (2012) Tobacco mosaic virus as a
605   new carrier for tumor associated carbohydrate antigens. Bioconjugate chemistry
606   23, 1694-1703.

607   21. Smith, M. L., Corbo, T., Bernales, J., Lindbo, J. A., Pogue, G. P., Palmer, K. E. and
608   McCormick, A. A. (2007) Assembly of trans-encapsidated recombinant viral
609   vectors engineered from Tobacco mosaic virus and Semliki Forest virus and
610   their evaluation as immunogens. Virology 358, 321-333.
611   22. Lundstrom, K. (2003) Semliki Forest virus vectors for gene therapy. Expert
612   opinion on biological therapy 3, 771-777.
613   23. Mahraj, P. D., Mallajosyula, J. K., Lee, G., Thi, P., Zhou, Y., Kearney, C. M. and
614   McCormick, A. A. ((accepted, 2014)) Nanoparticle encapsidation of Flock House
615   virus by auto assembly of Tobacco Mosaic virus coat protein. International
616   Journal of Molecular Sciences.
617   24. Johnson, K. L. and Ball, L. A. (1999) Induction and maintenance of
618   autonomous flock house virus RNA1 replication. Journal of virology 73, 7933-
619   7942.
620   25. Selling, B. H., Allison, R. F. and Kaesberg, P. (1990) Genomic RNA of an insect
621   virus directs synthesis of infectious virions in plants. Proceedings of the National
622   Academy of Sciences of the United States of America 87, 434-438.
623   26. Price, B., Roeder, M. and Ahlquist, P. (2000) DNA-Directed Expression of
624   Functional Flock House Virus RNA1 Derivatives in Saccharomyces cerevisiae,
625   Heterologous Gene Expression, and Selective Effects on Subgenomic mRNA
626   Synthesis. Journal of virology 74, 11724–11733.
627   27. Lindbo, J. A. (2007) High-efficiency protein expression in plants from
628   agroinfection-compatible Tobacco mosaic virus expression vectors. BMC
629   biotechnology 7, 52.
630   28. Turner, D. R. and Butler, P. J. (1986) Essential features of the assembly origin
631   of tobacco mosaic virus RNA as studied by directed mutagenesis. Nucleic acids
632   research 14, 9229-9242.
633   29. Liu, Z. and Kearney, C. M. (2010) An efficient Foxtail mosaic virus vector
634   system with reduced environmental risk. BMC biotechnology 10, 88.
635   30. Dasgupta, R., Cheng, L. L., Bartholomay, L. C. and Christensen, B. M. (2003)
636   Flock house virus replicates and expresses green fluorescent protein in
637   mosquitoes. Journal of General Virology 84, 1789-1797.
638   31. Price, B. D., Ahlquist, P. and Ball, L. A. (2002) DNA-Directed Expression of an
639   Animal Virus RNA for Replication-Dependent Colony Formation in
640   Saccharomyces cerevisiae. Journal of virology 76, 1610-1616.
641   32. Scholthof, H. B. (2006) The Tombusvirus-encoded P19: from irrelevance to
642   elegance. Nat Rev Microbiol 4, 405-411.
643   33. Ball, L. A., Amann, J. M. and Garrett, B. K. (1992) Replication of Nodamura
644   Virus after Transfection of Viral-Rna into Mammalian-Cells in Culture. Journal of
645   virology 66, 2326-2334.
646   34. Hwang, D. J., Roberts, I. M. and Wilson, T. M. (1994) Expression of tobacco
647   mosaic virus coat protein and assembly of pseudovirus particles in Escherichia
648   coli. Proceedings of the National Academy of Sciences of the United States of
649   America 91, 9067-9071.

650   35. Sleat, D. E., Gallie, D. R., Watts, J. W., Deom, C. M., Turner, P. C., Beachy, R. N.
651   and Wilson, T. M. (1988) Selective recovery of foreign gene transcripts as virus-
652   like particles in TMV-infected transgenic tobaccos. Nucleic acids research 16,
653   3127-3140.
654   36. Sacher, R., French, R. and Ahlquist, P. (1988) Hybrid brome mosaic virus
655   RNAs express and are packaged in tobacco mosaic virus coat protein in vivo.
656   Virology 167, 15-24.
657   37. Annamalai, P., Rofail, F., Demason, D. A. and Rao, A. L. (2008) Replication-
658   coupled packaging mechanism in positive-strand RNA viruses: synchronized
659   coexpression of functional multigenome RNA components of an animal and a
660   plant virus in Nicotiana benthamiana cells by agroinfiltration. Journal of virology
661   82, 1484-1495.
662   38. Rao, A. L. (2006) Genome packaging by spherical plant RNA viruses. Annual
663   review of phytopathology 44, 61-87.
664   39. Wilson, T. M. and McNicol, J. W. (1995) A conserved, precise RNA
665   encapsidation pattern in Tobamovirus particles. Archives of virology 140, 1677-
666   1685.
667   40. Abel, P. P., Nelson, R. S., De, B., Hoffmann, N., Rogers, S. G., Fraley, R. T. and
668   Beachy, R. N. (1986) Delay of disease development in transgenic plants that
669   express the tobacco mosaic virus coat protein gene. Science 232, 738-743.
670   41. Lindenbach, B. D., Sgro, J. Y. and Ahlquist, P. (2002) Long-Distance Base
671   Pairing in Flock House Virus RNA1 Regulates Subgenomic RNA3 Synthesis and
672   RNA2 Replication. Journal of virology 76, 3905-3919.
673   42. Sztuba-Solinska, J., Stollar, V. and Bujarski, J. J. (2011) Subgenomic messenger
674   RNAs: mastering regulation of (+)-strand RNA virus life cycle. Virology 412, 245-
675   255.
676   43. Phua, K. K., Nair, S. K. and Leong, K. W. (2014) Messenger RNA (mRNA)
677   nanoparticle tumour vaccination. Nanoscale 6, 7715-7729.
678   44. Weiner, D. B. (2013) RNA-based vaccination: sending a strong message.
679   Molecular therapy : the journal of the American Society of Gene Therapy 21, 506-
680   508.
681   45. Eckerle, L. D., Albarino, C. G. and Ball, L. A. (2003) Flock House virus
682   subgenomic RNA3 is replicated and its replication correlates with
683   transactivation of RNA2. Virology 317, 95-108.
684   46. Bonehill, A., Heirman, C., Tuyaerts, S., Michiels, A., Breckpot, K., Brasseur, F.,
685   Zhang, Y., van der Bruggen, P. and Thielemans, K. (2004) Messenger RNA-
686   Electroporated Dendritic Cells Presenting MAGE-A3 Simultaneously in HLA Class
687   I and Class II Molecules. The Journal of Immunology 172, 6649-6657.
688   47. Van Tendeloo, V. F., Ponsaerts, P., Lardon, F., Nijs, G., Lenjou, M., Van
689   Broeckhoven, C., Van Bockstaele, D. R. and Berneman, Z. N. (2001) Highly
690   efficient gene delivery by mRNA electroporation in human hematopoietic cells:
691   superiority to lipofection and passive pulsing of mRNA and to electroporation of
692   plasmid cDNA for tumor antigen loading of dendritic cells. Blood 98, 49-56.

693   48. Tkachenko, A. G., Xie, H., Coleman, D., Glomm, W., Ryan, J., Anderson, M. F.,
694   Franzen, S. and Feldheim, D. L. (2003) Multifunctional gold nanoparticle-peptide
695   complexes for nuclear targeting. J Am Chem Soc 125, 4700-4701.
696   49. Oliveira, S., van Rooy, I., Kranenburg, O., Storm, G. and Schiffelers, R. M.
697   (2007) Fusogenic peptides enhance endosomal escape improving siRNA-induced
698   silencing of oncogenes. International journal of pharmaceutics 331, 211-214.
699   50. Erazo-Oliveras, A., Muthukrishnan, N., Baker, R., Wang, T.-Y. and Pellois, J.-P.
700   (2012) Improving the Endosomal Escape of Cell-Penetrating Peptides and Their
701   Cargos: Strategies and Challenges. Pharmaceuticals 5, 1177-1209.

702

703

704   Figure Legends

705   **FIG 1** FHV viral vector constructs for expression in mammalian cells. (A) Two

706   constructs, C2 and C4, differing in the insertion site for eGFP. B2, FHV

707   silencing suppressor; Rbz, HDV ribozyme for precise viral RNA 3' end

708   excision. (B) Expression of T7/FHV-C2-GFP (left) and T7/FHV-C4-GFP (right)

709   in BHK21 cells.

710

711   **FIG 2** FHV viral vector constructs for expression in plants. The C2 and C4

712   constructs from Figure 1 were provided with the 35S plant expression

713   promoter and the TMV origin of assembly (Oa) to allow for encapsidation. (A)

714   In the C2 series, TMV-Oa was added at different positions in C2-o1, and -o2,

715   and in -o3 the eGFP native C terminal stop codon was preserved. B2' stands

716   for the B2 ORF C-terminal remaining after eGFP insertion. (B) The C4-2sg

717   has a duplicated subgenomic promoter to express unfused versions of eGFP

718   and B2 silencing suppressor. The eGFP ORF is between the duplicated

719   subgenomic promoters in C4-2sg, but follows the final subgenomic promoter

720   in 2sg2 construct. The 2sg2 constructs retain the B2 C-terminus (B2'')

721   following the eGFP ORF to mimic the 3' end of the native FHV. (C) The

722   FECT/TMVCP construct and the JL6/p19 were used as co-agroinoculants

723   and provided coat protein and silencing suppressor, respectively.

724

725   **FIG 3** eGFP expression from constructs from Figure 2. Agroinoculated leaves

726   of *Nicotiana benthamiana* were examined, 7 dpi, under blue light with visible

727   light to outline leaf shape. 35S/FHV-C2 inoculated alone or with p19 silencing

728   suppressor. FECT-eGFP is general high expression positive control. F1DI (+/-

729   p19) is a positive control for FHV/GFP expression and comprises FHV RNA1

730   plus a defective interfering construct of RNA2. All other inoculations included

731   p19 unless otherwise mentioned. 2sg2KSS construct is included in the

732   supplementary data. All other designations as in Figure 2.

733

734   **FIG 4** eGFP expression in plants by FHV constructs and in 1-step and 2-step

735   inoculation procedures. (A) eGFP fluorometry of *N. benthamiana*

736   agroinoculated with various FHV constructs. p19, mock inoculation with p19

737   only; FECT-eGFP, high expression positive control; 1-step and 2-step, co-

738   agroinoculation or delayed TMVCP agroinoculation. Four replicates each

739   treatment, except 15 replicates for 1-step and 2-step treatments. (B) eGFP

740   expression compared in 1-step and 2-step agroinoculation procedures. FHV-

741   C2-o3 without any FECT-TMV was also inoculated as a control.

742

743   **FIG 5** Expression of TMV CP by FECT plant viral vector. Lane a, FECT

744   expressing TMV CP; Lane b, TMV vector JL24 (23) expressing CP and

745   eGFP. Both agroinoculations in *N. benthamiana* included p19 silencing

746   suppressor. Far left lane: protein marker (NEB # P7708) with sizes in kDa

747   indicated.

748

749   **FIG 6** Co-infection of plant cells by FHV and FECT viral vectors. (A) *N.*

750   *benthamiana* plants were agroinoculated with p19 plus (left to right)

751   35S/FHVC2-o3/GFP, FECT/DsRed or both vectors. (B) Protoplasts made

752   from 4 dpi leaves coagroinoculated with FHV-eGFP/FECT-DsRed (right leaf

753   in (A)) were visualized for eGFP and DsRed fluorescence, showing the

754   majority of the FHV-eGFP infected cells were also infected with FECT.

755

756   **FIG 7** TEM of *in vitro* and *in planta* produced nanoparticles. (A) *In vitro*

757   assembled FHVOa. (B) *In vitro* assembled SFVOa (C) *in planta* assembled

758   FHV-C2-o3 (CP provided by FECT/TMVCP). 100 nm bars indicated.

759

760   **FIG 8** *In vivo* analysis of FHV vaccine potency. Balb/C Mice (n = 3) were

761   vaccinated 3 times, two weeks apart with indicated amounts (15 or 30 µg

762   protein) of TMV encapsidated FHV-eGFP, produced either *in vitro* by mixing

763   RNA and coat protein, or *in planta* by co-expression of RNA and coat protein

764   after agroinfiltration. PBS was used as a negative control, and *in vitro*

765   encapsidated SFV-eGFP or 15ug of eGFP protein was used as a positive

766   control. ELISA analysis was used to determine anti-eGFP IgG titers on sera

767   collected at 10 d after either vaccine 2 (pV2) or after vaccine 3 (pV3). Titers

768   were measured against a known quantity of anti-eGFP standard (Vector

769   labs), and shown as mean +/- SEM using GraphPad Prism. Statistical

770   analysis of differences between PBS and vaccine groups after vaccine 3 was

771   evaluated by one-tailed t-test. The asterisk indicates statistically significant

772   difference from PBS control.

773

774

775

776

777

778

779

780

781

782

783

784

A.

T7/FHV-C-GFP

B.
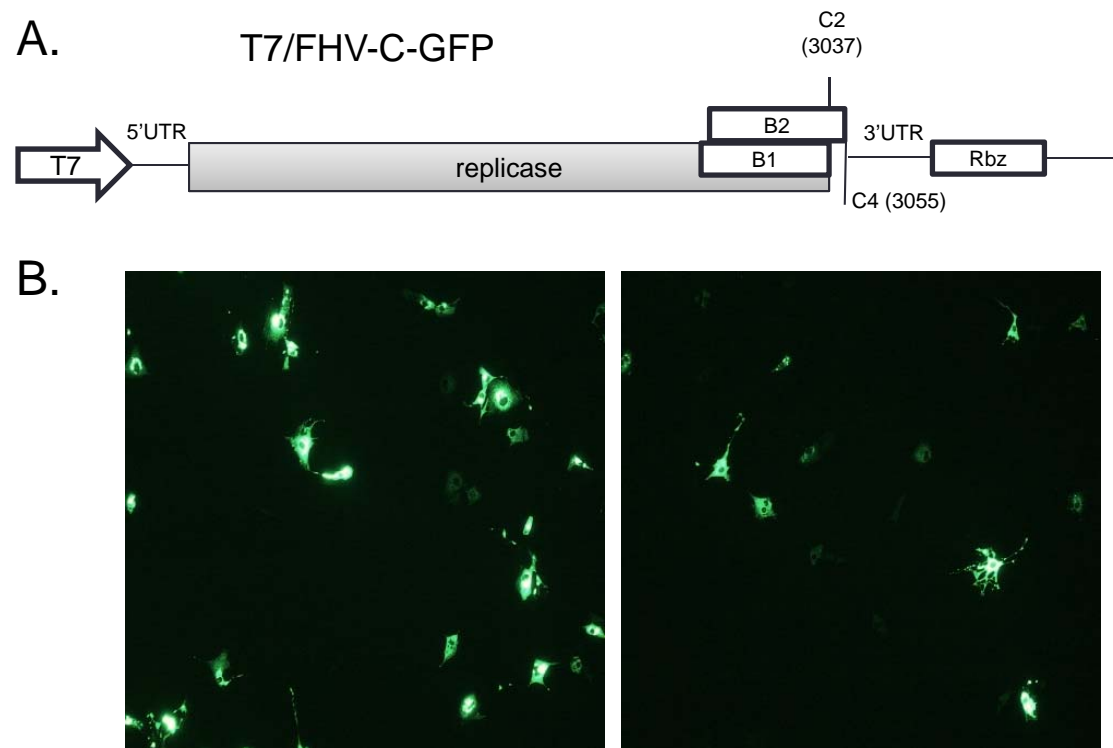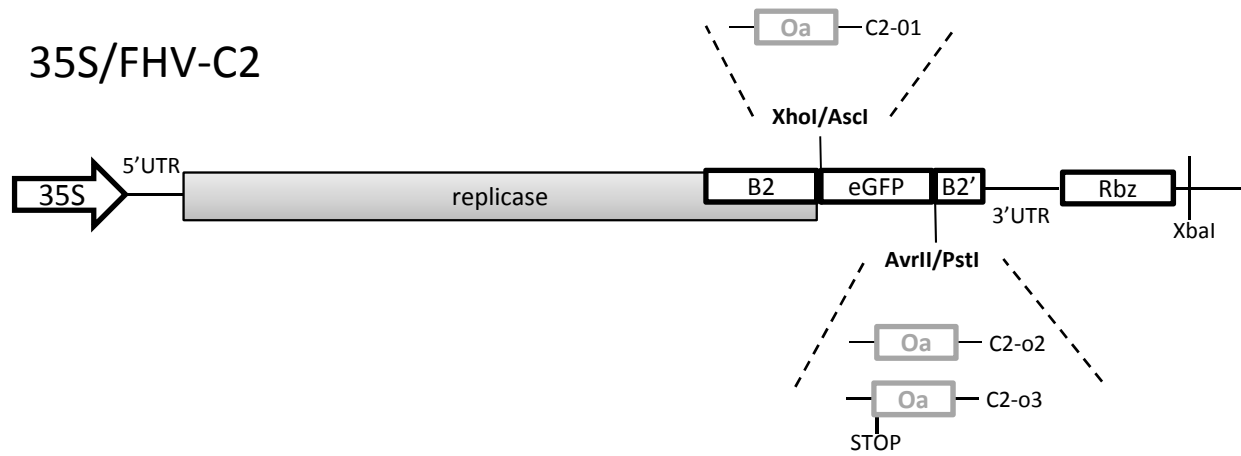
Figure 1

35S/FHV-C2

Figure 2A

35S/FHV-C4-2sg
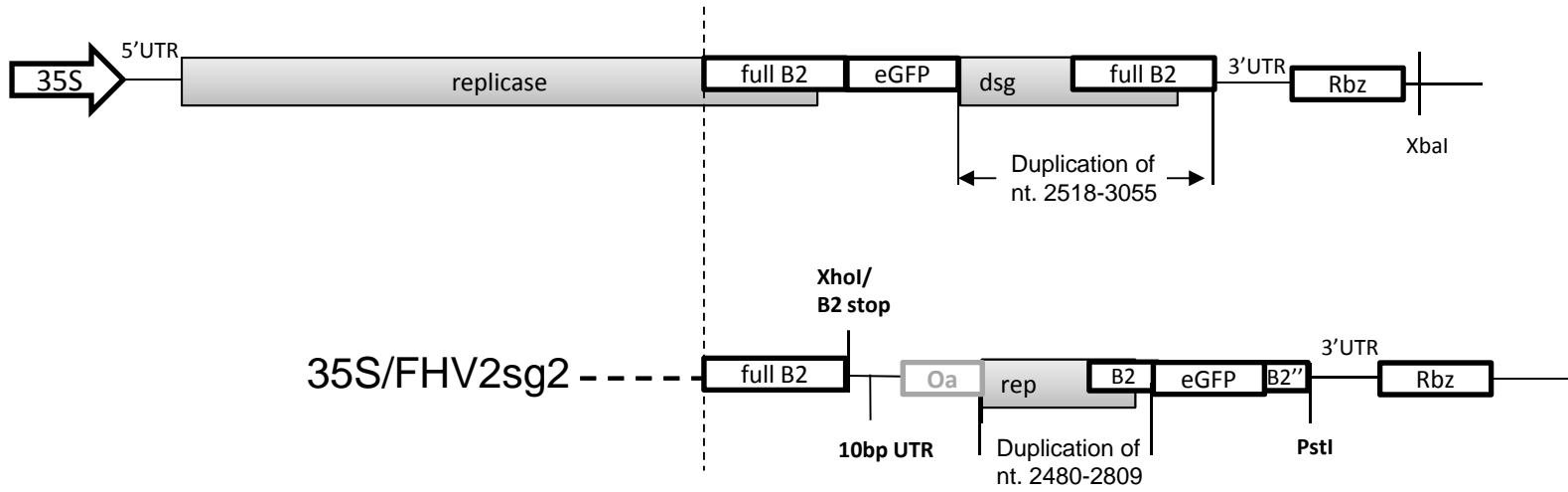
Figure 2B

FECT/TMVCP

JL6/p19

Figure 2C

C2 alone   C2 + p19   FECT-EGFP control

2sg2   2sg2KSS   F1DI no p19   F1DI

C4   C2

C2-o1   C2-o2   C2-o3
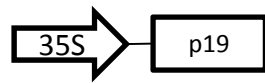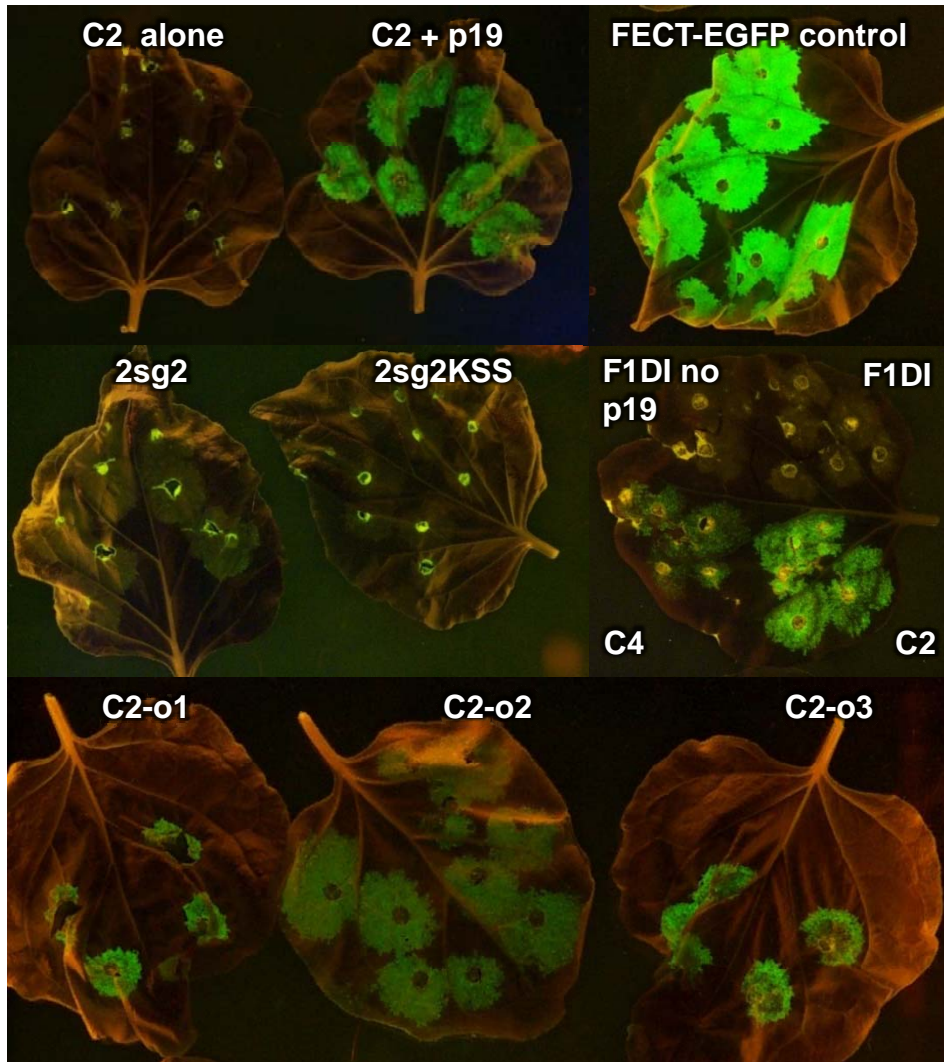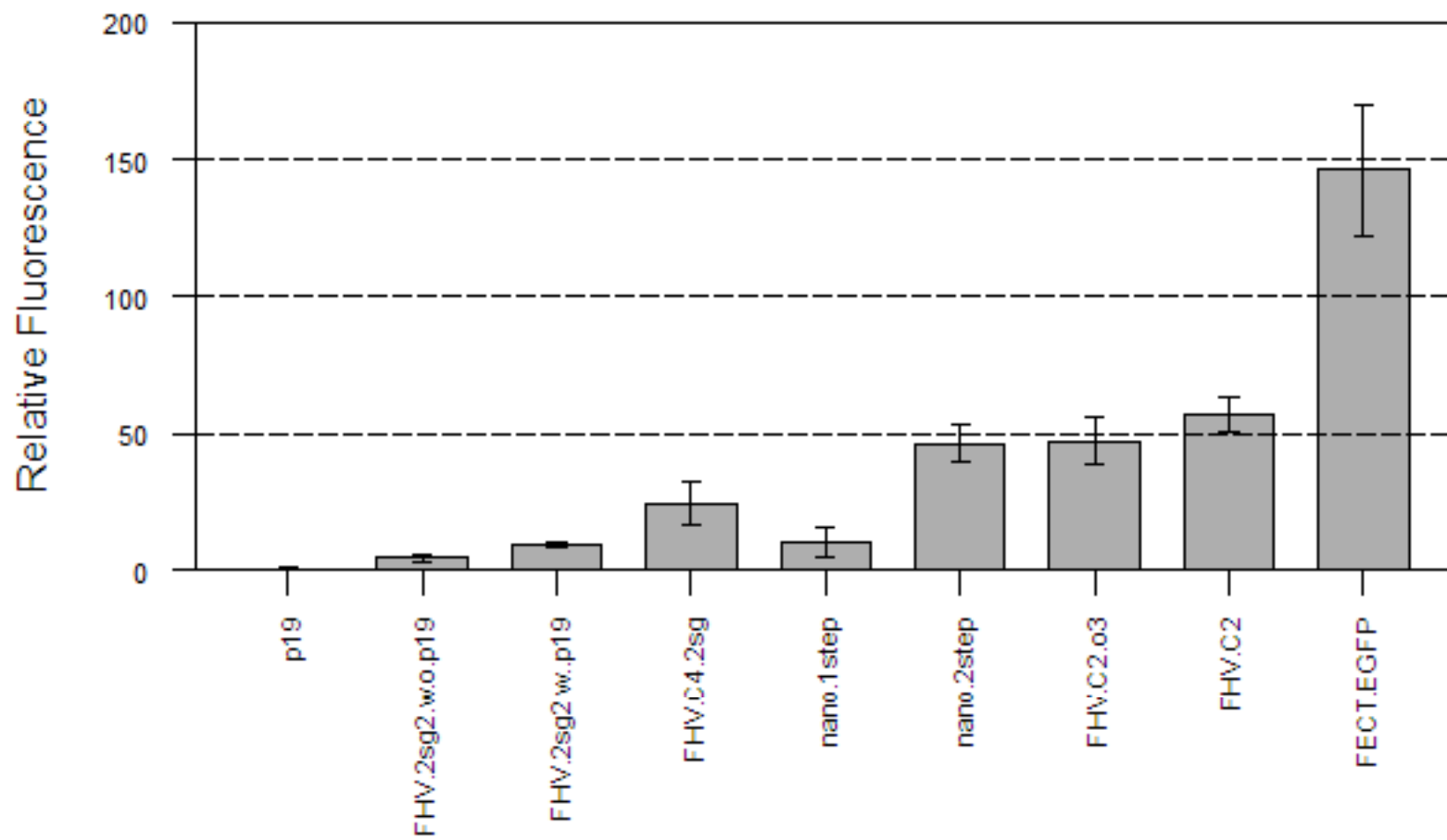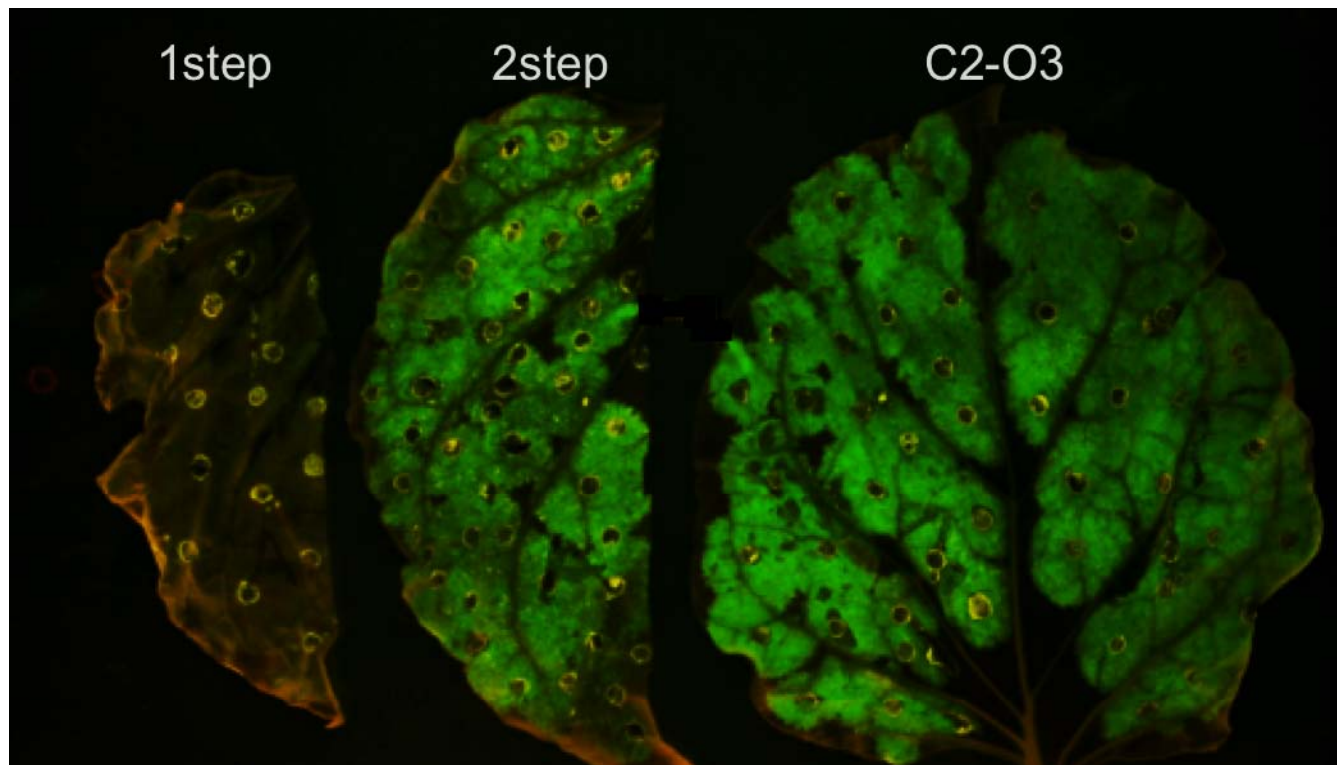
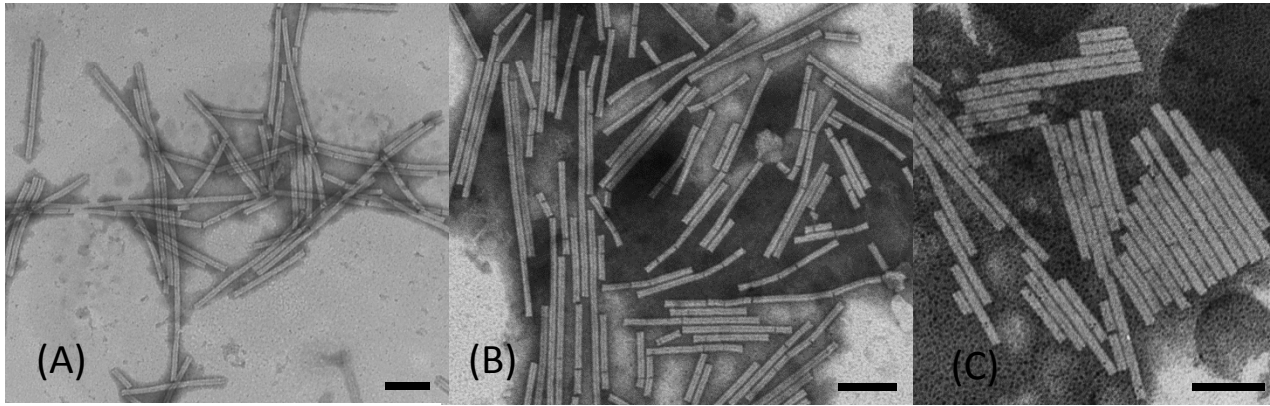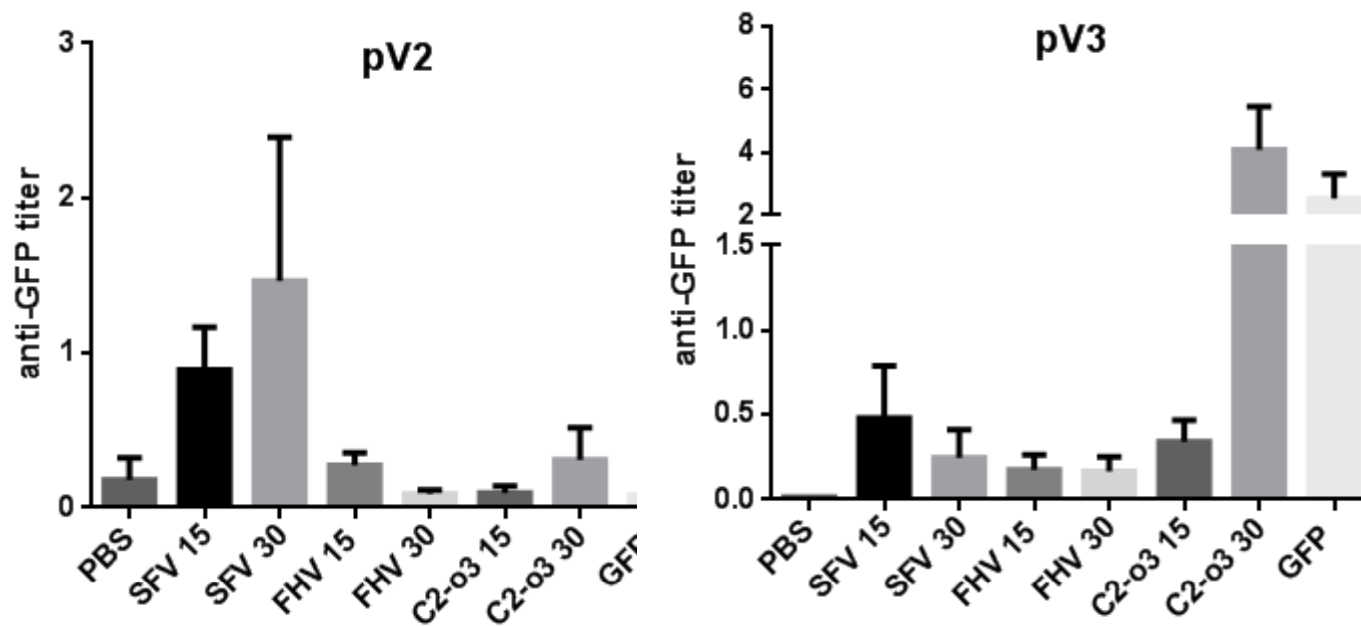**Figure 3**

Figure 4A

Figure 4B
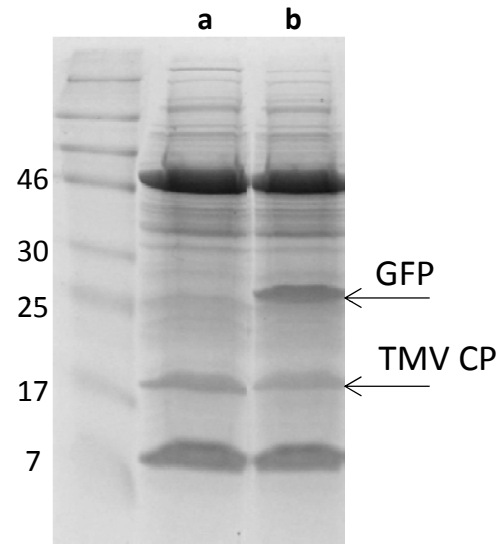
Figure 5
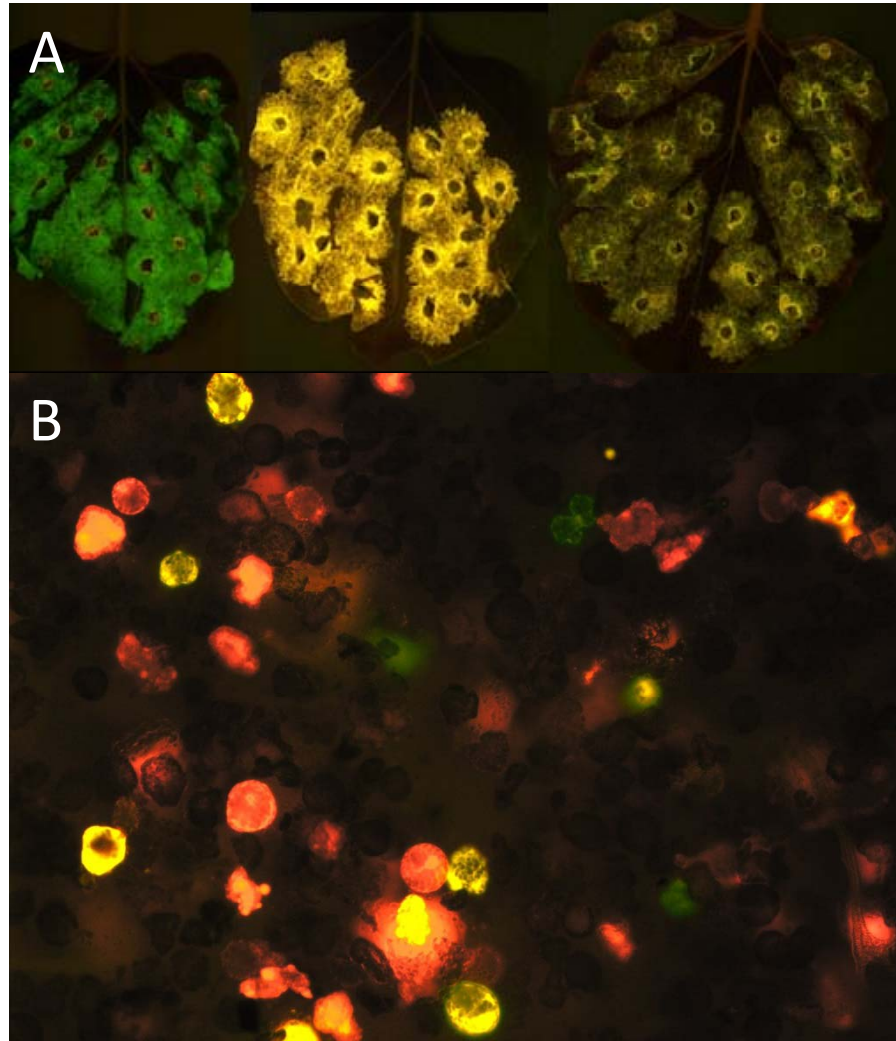
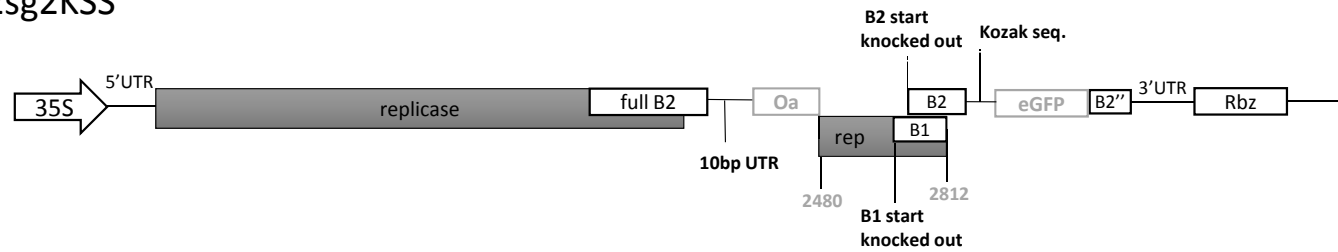**Figure 6**

Figure 7

one tailed t-test vs PBS:
SFV 15 p=0.224
SFV 30 p=0.116
FHV 15 p=0.104
FHV 30 p=0.110
C2-o3 15   p=0.063
*C2-o3 30   p=0.048
*GFP   p=0.047

Figure 8

FHV2sg2KSS

Suppl. Fig 1: In seek to further aid eGFP expression, a 35S/FHV-2sg2KSS construct was built, in which the B1 and B2 start codons were knocked out and an ATG with strong Kozak context (CCACC ATG) was placed at the start of the eGFP ORF, resulting in an eGFP/B2 fusion with only a short B2 portion C-terminal to the eGFP.

FHV C2 + FECT TCP   FHV C2 only
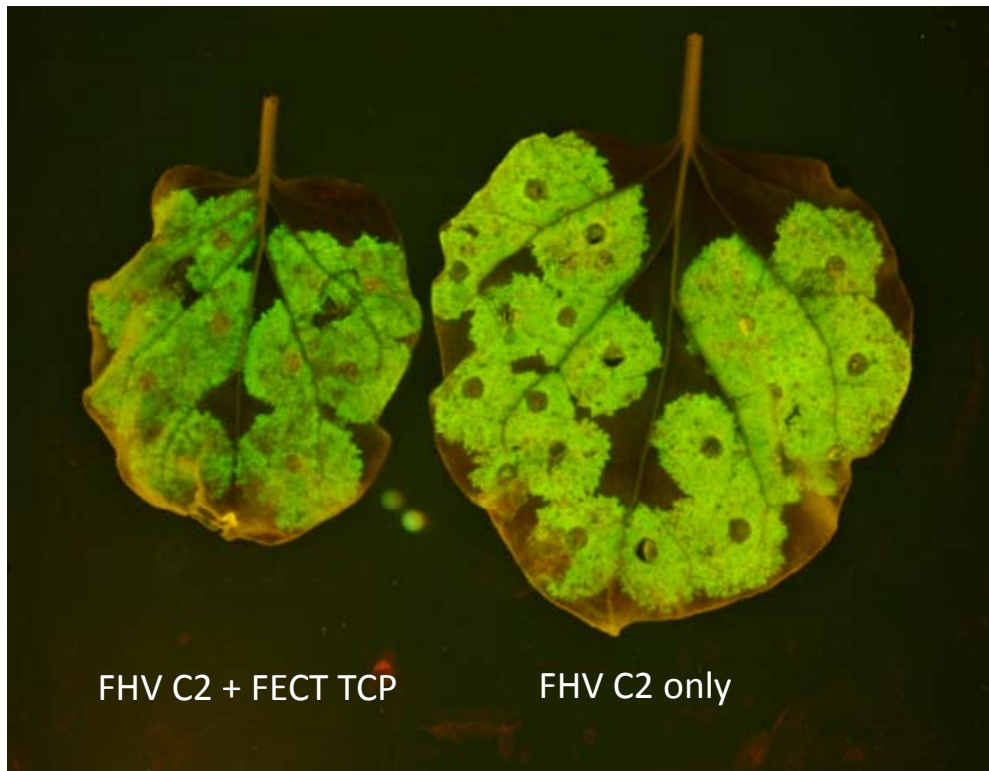
Suppl. Fig 2: In order to determine whether FECT virus will interfere with FHV replication in planta, FHVC2/GFP lacking the Oa sequence was co-inoculated with FECT-TCP and compared with FHVC2/GFP in the absence of FECT-TCP. Fluorescence was similar in the presence (left) or absence (right) of FECT coinfection. This confirmed the reduction of fluorescence by coinfection with FHVC2/GFP containing the TMV Oa and FECT-TCP expressing coat protein is due to the hypothesized classical coat protein resistance. All experiments were carried out with p19 co-inoculation